

Towards Modelling the Solar Axion Spectrum with Self Consistent PIC–MC Plasma Simulations

Ahmed Ayidh Alsulami¹, Pablo J. Bilbao¹, Miles Radford¹, Thomas Grismayer², Bertrand Martinez^{3,4}, Luis O. Silva², Robert Bingham^{5,6}, and Gianluca Gregori¹

¹Department of Physics, University of Oxford, Parks Road, Oxford OX1 3PU, United Kingdom.

²GoLP/Instituto de Plasmas e Fusão Nuclear, Instituto Superior Técnico, Universidade de Lisboa, Lisboa, Portugal.

³CEA, DAM, DIF, F-91297 Arpajon, France.

⁴Université Paris-Saclay, CEA, Laboratoire Matière en Conditions Extrêmes, F-91680 Bruyères-le-Châtel, France.

⁵Department of Physics, University of Strathclyde, Glasgow G4 0NG, United Kingdom.

⁶Rutherford Appleton Laboratory, STFC, Didcot OX11 0QX, United Kingdom.

The implementation of processes occurring in a Coulomb field, as well as binary collisions, within PIC codes is typically achieved by integrating a Monte Carlo (MC) scheme into the standard PIC cycle (Figure 1). The MC algorithm is executed in every simulation cell at each timestep and is invoked before the completion of the PIC loop. The method consists of evaluating the probability of a given process during the particle-pushing stage according to

$$P = \sigma_{tot} c n_t \Delta t \quad (1)$$

where σ_{tot} is the total cross section of the process under consideration, c is the speed of light, n_t is the number density of target particles, and Δt is the simulation timestep.

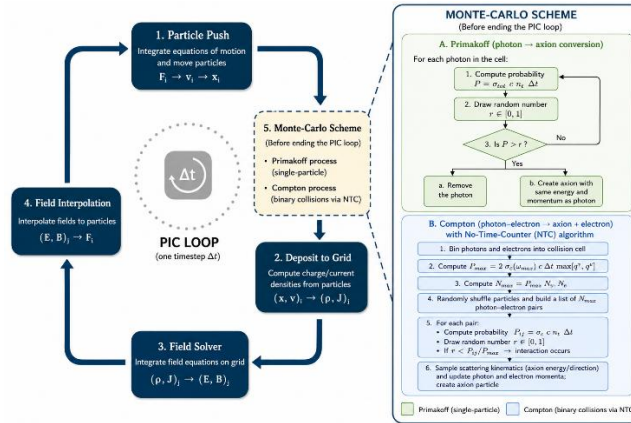


Figure 1: Schematic of the PIC cycle and the Monte Carlo modules used for axion production. The standard PIC loop consists of particle pushing, charge and current deposition, field solving, and field interpolation. Before completion of each timestep, Monte Carlo processes are evaluated. Primakoff photon–axion conversion is treated as a single-particle stochastic process based on a local conversion probability, whereas axion production through Compton scattering is implemented as a binary collision process using the No-Time-Counter (NTC) algorithm.

The probability P is computed and compared with a uniformly distributed random number to determine whether an interaction occurs. In this paper, we describe the implementation of Primakoff and Compton-like axion production processes in plasmas. Both processes are incorporated into a PIC Monte Carlo (PIC-MC) framework enabling their self-consistent treatment within the PIC simulation cycle.

I. Numerical Implementation of Primakoff Axion Production

For the Primakoff process, the probability of photon–axion conversion is evaluated for every photon in the plasma at each simulation timestep. This calculation is performed within the photon pusher using the local plasma conditions and the selected Primakoff rate model, either non-screened or screened according to the associated cross section [1]. If the computed probability exceeds a sampled random number from a uniform distribution, the photon is removed from the simulation and replaced by an axion, created in situ with the appropriate energy and momentum. Because the relevant cross section is typically very small, we introduce a boosting factor to artificially enhance the cross section, thereby increasing the resulting probabilities to values that are statistically meaningful for comparison with a random number in the interval $[0, 1]$. This technique is well established for rare processes and is valid in PIC codes, where each simulation particle represents a weighted macro-particle. The particle weight in PIC codes is defined as

$$q = \frac{N_{real\ particles}}{N_{macro\ particles}}. \quad (2)$$

To preserve correct normalization, the weight of each macro axion generated via this method is divided by the boosting factor, consequently, each simulated macro axion represents only a fraction of a physical axion.

II. Numerical Implementation of Compton Axion Production

For the Compton conversion of photons into axions, we adopt the No-Time-Counter (NTC) algorithm developed by Bird [2] to model binary collisions. Unlike the Primakoff process, where the interaction probability is evaluated independently for each photon within the photon pusher, Compton production requires explicit treatment of photon–electron interactions. A direct Monte Carlo implementation would require considering all possible photon–electron pairs, resulting in a computational cost proportional to $N_e N_\gamma$, where N_e and N_γ are the numbers of electrons and photons, respectively. For realistic particle populations, this quickly becomes computationally prohibitive. The NTC algorithm circumvents this difficulty by constructing a statistically representative subset of candidate collision pairs rather than evaluating all possible interactions. The Monte Carlo collision procedure is then applied only to this reduced set of pairs, preserving the correct collision statistics while substantially reducing the computational cost. As a result, the algorithm scales efficiently to large particle numbers and is well suited for PIC–MC simulations involving binary interaction processes.

The NTC method proceeds as follows. We begin by calculating the maximum number of potential interacting photon–electron pairs as

$$N_{max} = P_{max} N_\gamma N_e \quad (3)$$

where N_γ and N_e are the total number of photons and electrons, respectively, within the interaction cell, and P_{\max} is the maximum interaction probability. For the Compton-type conversion of photons into axions, the maximum collision probability used by the NTC algorithm is given by

$$P_{\max} = 2 \sigma_c(\omega_{\max}) c \Delta t \max [q_\gamma^i, q_e^j] N_e \quad (4)$$

where $\sigma_c(\omega_{\max})$ is the axion Compton cross section [1] evaluated at the maximum photon energy ω_{\max} within the interaction cell, and $\max [q_\gamma^i, q_e^j]$ is the maximum macro-particle weight, expressed in density units, among all photons and electrons in that cell. The factor of two provides a conservative upper bound on the collision probability and accounts for possible relativistic enhancement of the interaction rate. To ensure applicability in relativistic plasma environments, the photon energy used in the evaluation of the Compton cross section is Lorentz transformed into the electron rest frame. The resulting Lorentz-boosted photon energy is then used when computing the collision probability and determining whether a photon–electron pair undergoes axion-producing Compton conversion. Using Eq.3, we determine the maximum number of photon–electron pairs and store them in a list. For each pair, we apply the MC method described earlier by comparing P/P_{\max} with a uniformly sampled random number, where P is computed using Eq.1 with the axion Compton cross section.

III. Validation: Benchmarking Axion Production in the Solar Core

We report the solar energy distributions of Primakoff and Compton axions in Fig.2. In both cases, the resulting distribution does not simply mirror the photon distribution. For the Primakoff process, the energy distribution peaks at $E_{a,p}/T = 3.3$, with a mean energy of $\langle E_{a,p}/T \rangle = 4.3$. For the Compton process, the peak occurs at $E_{a,c}/T = 4.0$, with a mean energy of $\langle E_{a,c}/T \rangle = 4.8$. By contrast, the photon distribution peaks at $E_\gamma/T = 1.6$, with a mean energy of $\langle E_\gamma/T \rangle = 2.7$, highlighting that the axion distributions are significantly shifted due to the energy dependence of the production cross sections. These numerical values are in good agreement with the analytical predictions reported by Raffelt [1] for solar-core conditions.

Worth noting is that the Compton spectrum is shifted toward higher energies relative to the Primakoff spectrum, consistent with the additional ω^2 dependence of the Compton cross section. The total axion yield is also significantly larger for Compton production, about 1.5 orders of magnitude higher, despite the use of the same multiplicative enhancement factor in both simulations. Under the benchmark solar-core conditions considered here, this indicates that the implemented Compton channel produces axions more efficiently than the Primakoff channel.

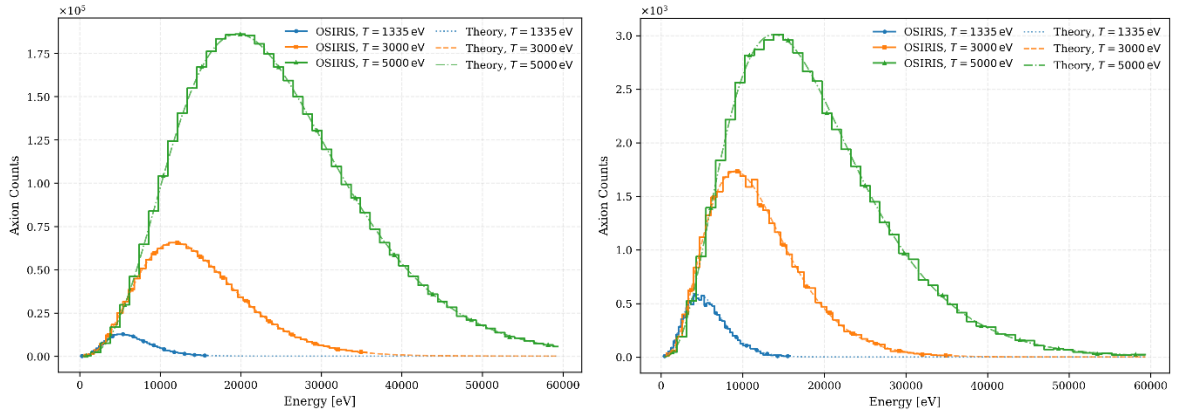


Figure 2: Comparison between the analytical predictions and OSIRIS simulations for axion production through (a) Primakoff conversion and (b) Compton scattering at three plasma temperatures. The analytical spectra are scaled to the corresponding simulation yields to facilitate comparison of the spectral shape. Good agreement is observed across the full energy range, validating the numerical implementation of both production channels.

IV. Summary

The resulting axion spectra show good agreement with the corresponding analytical predictions, validating the numerical implementation of both the Primakoff and Compton production channels. The framework enables direct calculations of axion energy spectra, production rates, and associated energy-loss rates within a self-consistent PIC–MC environment. Furthermore, the implementation can be naturally extended to relativistic plasma regimes, where PIC methods are particularly well suited. The coupling constants considered in this work correspond to axion masses of order 1eV. In this mass range, axions possess mean free paths that are significantly larger than the characteristic size of the simulation domain and the solar plasma itself. Consequently, axion reabsorption is negligible, and inverse processes may be safely neglected. This implementation represents the first step in a series of future works aimed at incorporating axion physics into PIC frameworks. Future developments could focus on predictive modeling of axion production in plasmas with instabilities and on investigating nonlinear phenomena, including the amplification of axion fields.

References

- [1] Georg G. Raffelt. Astrophysical axion bounds diminished by screening effects. *Phys. Rev. D*, 33:897–909, Feb 1986.
- [2] G. A. Bird. Perception of numerical methods in rarefied gasdynamics. *Progress in Astronautics and Aeronautics*, 117:211–226, 1989.